Organic & Biomolecular Chemistry

A silicon rhodamine 1,2-dioxetane chemiluminophore for in vivo near-infrared imaging

Journal:	*Organic & Biomolecular Chemistry*
Manuscript ID	OB-COM-12-2024-002002.R1
Article Type:	Communication
Date Submitted by the Author:	14-Jan-2025
Complete List of Authors:	Osman, Rokia; Southern Methodist University Haris, Uroob; Southern Methodist University, Chemistry Cabello, Maidileyvis; Southern Methodist University Mason, Ralph; The University of Texas at Dallas, Southwestern Medical Center Lippert, Alexander; Southern Methodist University,

COMMUNICATION

A silicon rhodamine 1,2-dioxetane chemiluminophore for in vivo near-infrared imaging

Received 00th January 20xx,
Accepted 00th January 20xx

DOI: 10.1039/x0xx00000x

Rokia Osman,[a,†] Uroob Haris,[a,†] Maidileyvis C. Cabello,[a,†] Ralph P. Mason,[b] and Alexander R. Lippert[*a]

Near-infrared (NIR) chemiluminescent probes have attracted increasing attention in recent years due to their attractive properties for in vivo imaging. Herein, we developed a NIR chemiluminophore silicon rhodamine (SiRCL-1) based on the intramolecular energy transfer process from excited state benzoate to a silicon rhodamine emitter under aqueous conditions. SiRCL-1 exhibited dual emission peaks at 540 nm and 680 nm with a high signal penetration through tissue at 680 nm (>30 mm) and long-lasting *in vivo* luminescence (>50 min), demonstrating its significance as a chemiluminescence scaffold for biological application.

Chemiluminescence is a photochemical phenomenon wherein light is generated *via* a chemical reaction.[1] The decomposition of 1,2-dioxetanes, following a chemically initiated electron exchange luminescence (CIEEL) mechanism, is one such reaction that forms the basis of a popular class of non-enzymatic chemiluminescent molecular bioimaging agents.[2] Unlike fluorescence imaging, chemiluminescence imaging features a response independent of light absorption, thus bypassing background signal from autofluorescence, and enabling higher imaging sensitivity. In recent years, the repository of these triggerable 1,2-dioxetane probes which exhibit chemiluminescence emission in response to specific bioanalytes has rapidly grown[2–6] following demonstration of their *in vivo* use[7,8] and aqueous compatibility.[9,10] Indeed, chemiluminescence imaging now spans analytes including but not limited to, enzymes,[8,11] reactive nitrogen, oxygen, and sulphur species[12,13] (including recent advances towards organelle targeting),[14,15] protein interactions,[16] pH,[17,18] and hypoxia,[19,20] as well as multiplexed analyte detection systems.[21]

In order to further the *in vivo* applicability of these imaging agents, efforts are underway to shift their chemiluminescence emission from the conventional blue and green emission to the near infrared (NIR), which allows higher signal penetration through tissue and greater imaging depth.[22–24] Extension of π conjugation and introduction of push-pull systems have been explored as strategies to red-shift the emission of the benzoate decomposition product directly.[24,25] Another strategy to achieve red-shifted emission is the use of non-radiative energy transfer mechanisms. Chemiluminescence resonance energy transfer-based strategy (CRET) allows for fluorophores with energy transfer capabilities such as 1,2-dioxetanes to be paired to dyes with sensing capabilities providing ratiometric detection of analytes with the CRET pair, an advantageous property when compared to π-extended luminophores.[18] In this strategy, the excited state benzoate generated during the CIEEL process transfers energy to a covalently tethered red-emitting fluorophore based on spectral overlap of the luminophores.[26,27] Chemiluminescence platforms leveraging long distance singlet oxygen transfer (SOT) processes do not require spectral overlap and provide what is referred to as afterglow substrates. Most afterglow SOT-based probes are fabricated by separately loading precursors and photosensitizers into nanoparticles.[28,29,30] Previously, intramolecular energy transfer based NIR chemiluminescence has been reported for detection of hypoxia,[20] pH,[17,18] hydrazine,[31] and enzymes like ß-galactosidase.[32]

Energy transfer pairings of 1,2-dioxetanes with several NIR-emitting luminophores have been explored[26] (>600 nm) including quinone-cyanine,[32] dicyanoisophorone,[33] iridium complexes[20,27] and an aggregation-induced emission generating fluorophore.[31] However, limitations of these systems such as low brightness and challenging syntheses, leave room for exploration of synthetically accessible and high performing chemiluminescence energy transfer acceptors. Of NIR emitting fluorophores, silicon rhodamines (SiR)[34] in particular have been used extensively for development of triggerable fluorescent probes, owing to their photostability, and high quantum yield.[35] Turn-on fluorescent probes based on silicon rhodamine dyes

[a] *Department of Chemistry, Southern Methodist University, Dallas, TX 75275-0314 (USA)*
[b] *Prognostic Imaging Research Laboratory, Pre-clinical Imaging Section, Department of Radiology, UT Southwestern Medical Center, Dallas, TX 75390-9058 (USA)*
† These authors contributed equally.
Electronic Supplementary Information (ESI) available: Experimental procedures and supplementary figures. See DOI: 10.1039/x0xx00000x

have been reported for varied bioimaging applications in cells and *in vivo* such as detection of proteases,[36,37] endogenous peroxynitrite,[38] cellular lysosomal pH,[39] retinal hypoxia,[40] nitric oxide,[41,42] hypochlorous acid,[43,44] neuronal calcium ions,[45] and cellular zinc ions.[35] In comparison, reports of chemiluminescent probes incorporating this fluorescent emitter are, to the best of our knowledge, non-existent. Translation of these SiR based fluorogenic probes to their chemiluminescent counterparts could provide access to NIR imaging of a wide variety of analytes through tissue, thus furthering the applicability of chemiluminescent biosensing and analyte quantification.

Herein, we report a NIR silicon rhodamine based chemiluminophore, **SiRCL-1**, which undergoes CIEEL and exhibits efficient energy transfer from the excited state benzoate to the appended silicon rhodamine emitter in aqueous systems. We investigated the chemiluminescence decay kinetics, quantum yield of chemiluminescence, and demonstrated its imaging capabilities *in vivo*.

We designed **SiRCL-1** to consist of a chemiluminescent spiroadamantane 1,2-dioxetane scaffold with a free phenol, attached to a silicon rhodamine fluorophore *via* a piperazine based on previous success with this linker (Scheme 1).[20] Silicon rhodamine carboxylic acid **SiR**[18,46] was synthesized and modified with 1-Boc-piperazine through peptide coupling, and the enol ether moiety **2** containing an acrylate functionality was appended to the silicon rhodamine piperazine to furnish the dioxetane precursor **3** with a protected phenol. Gentle cleavage of the acetate group using ammonium acetate and subsequent reaction with singlet oxygen afforded the dioxetane **SiRCL-1**.

Scheme 1. Synthesis of **SiRCL-1**

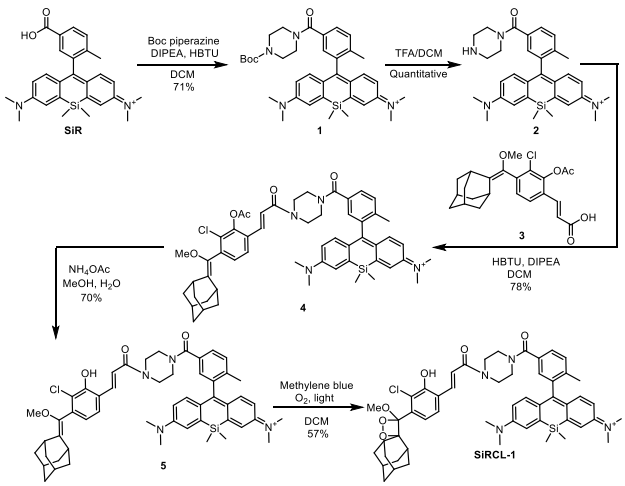

Following synthesis, we moved to characterizing spectroscopic properties of **SiRCL-1**. We found that the compound exhibited an absorbance maximum at 655 nm, and we verified that this spectrum overlaps with the emission of the energy donor, methyl acrylate dioxetane (Figure S1),[10] which is a requisite for resonance energy transfer (Figure 1A). We next tested the chemiluminescent response of **SiRCL-1**. In an acidic citrate buffer, where the compound exists as a phenol, no chemiluminescence emission was observed. Immediately after addition of NaOH, upon decomposition of the phenolate and CIEEL, chemiluminescence emission peaks at 540 nm and 680 nm were observed, corresponding to direct emission from the excited state benzoate and emission from the silicon rhodamine because of energy transfer, respectively (Figure 1B). To further characterize the pH dependence, the luminescence response to varying pH was studied. **SiRCL-1** showed no emission signal at pH below 5. A significant response was observed at pH 7.4, and maximum emission was reached and stayed relatively steady between pH 7–9 (Figure 1C,D). At pH 12, in 0.1 M NaOH the 540 nm peak rose drastically, and the 680 nm peak reduced in intensity, which could possibly indicate hydrolysis and cleavage of **SiR** from the compound (Figure S2A). Chemiluminescence emission was observed in PBS buffer with DMSO content as low as 5% (Figure S2B) and investigation with a commercially available Emerald II Enhancer solution showed an increase in 540 nm emission with a decrease in the 680 nm emission (Figure S2C). These studies showed that efficient chemiluminescence emission can be observed at physiological pH under aqueous conditions with a small amount of DMSO co-solvent.

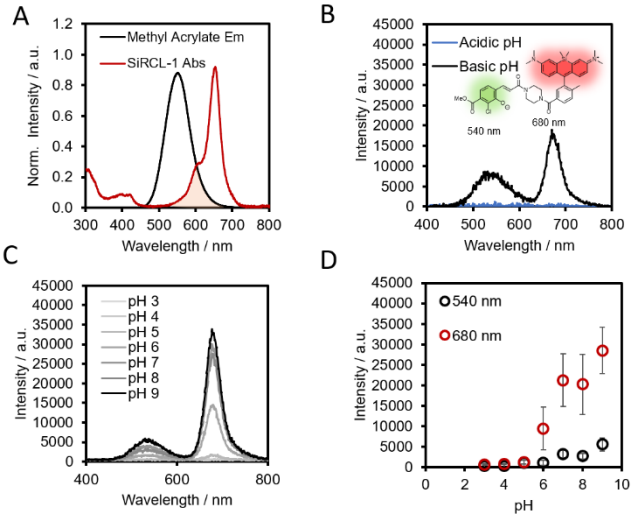

Figure 1. (A) Spectral overlap between chemiluminescence emission of methyl acrylate dioxetane and absorbance of **SiRCL-1**. (B) Chemiluminescence emission peaks at 540 nm (benzoate) and 680 nm (SiR) of 40 µM **SiRCL-1** with 20% DMSO in 100 mM citric acid buffer, pH 4.97 (acidic conditions), and immediately after basification to 200 mM NaOH (basic conditions). (C) Chemiluminescence emission traces of 20 µM **SiRCL-1** with 30% DMSO at pH 3–9. (D) Emission intensity of 20 µM **SiRCL-1** at 540 nm and 680 nm with varying pH with 30% DMSO. Error bars are ± S.D. with n = 3–5 independent replicates.

Through time course studies, we monitored the decay of chemiluminescence emission for **SiRCL-1** over a period of 60 min (Figure 2A). By fitting the intensity decay data at 540 nm and 680 nm to an exponential first order model, we determined the rate constant for the chemiluminescence decay *in vitro* to be 6.3 ± 0.91 x 10^{-3} s^{-1} and a half-life of chemiluminescence emission to be 111 ± 15 s (Figure 2B). The quantum yield was measured to be (3.9 ± 0.81) x 10^{-3} E mol^{-1} using a procedure modified from Baader et al.[47,48]

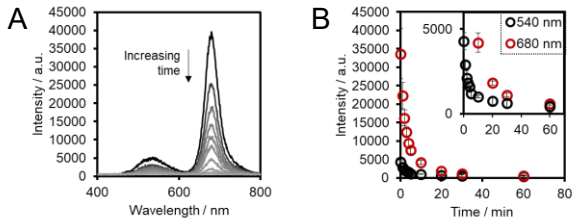

Figure 2. (A) Chemiluminescence emission time course scans of 20 µM **SiRCL-1** from 0 min to 60 min in PBS buffer (pH 7.4) with 30% DMSO. (B) Emission decay between 0 and 60 min for 20 µM **SiRCL-1** in PBS (pH 7.4) with 30% DMSO at 540 nm and 680 nm. Inset: Intensity axis scaled down for detailed view of 540 nm emission decay. Error bars are ± S.D. with n = 3 replicates.

To study the capability of **SiRCL-1** for *in vivo* imaging, we first examined the potential of the chemiluminescent signal to penetrate tissue using turkey deli slices as a tissue model. Stacks of turkey slices (slice thickness = 1.54 mm) were placed over an opaque 96-well microtiter plate loaded with the chemiluminescent reaction (100 µM **SiRCL-1** in 30% DMSO in PBS at pH 7.4). Emissions at 540 nm and 680 nm were measured through the thicknesses of tissue with 10 second exposure times (Figure 3A). With 0 slices of tissue, chemiluminescence emission at 540 nm and 680 nm were both clearly detected by the IVIS Spectrum imaging instrument (Figure 3A). With increasing thickness of the tissue stack, chemiluminescence emission was increasingly scattered and absorbed by the tissue. The shorter wavelength emission at 540 nm was detectable through up to 6 mm of tissue thickness, while the longer wavelength, NIR 680 nm signal was observed through even up to 30 mm of tissue thickness. This provided strong evidence for high tissue depth penetration of signal granted by energy transfer to the silicon rhodamine emitter.

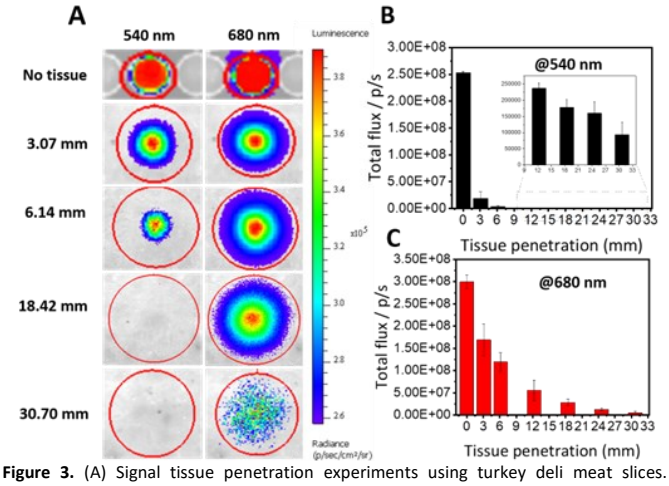

Figure 3. (A) Signal tissue penetration experiments using turkey deli meat slices. Chemiluminescence signal heatmap of 100 µM **SiRCL-1** in 30% DMSO/PBS (pH 7.4) was imaged through increasing tissue depth at 540 and 680 nm using an exposure time of 10 seconds. Dependence of total flux with tissue penetration at (B) 540 nm and (C) 680 nm. Error bars are ± S.D. with n = 3 independent trials.

Encouraged by high signal depth penetration of **SiRCL-1** chemiluminescence, we tested the potential of this system for *in vivo* chemiluminescence imaging. Live female nude mice aged 3 months were injected with 100 µM **SiRCL-1** (20 µL, 100 mM PBS, pH 7.4, 10% DMSO) into the peritoneal cavity and immediately imaged using IVIS system with 680 nm and 540 nm bandpass filters and 10 second exposure times (Figure 4). **SiRCL-1** showed a strong signal at 680 nm *in vivo*, which was detectable for up to 50 min after injection The decay of the emission intensity over time was monitored at both wavelengths (Figure 4B). The total flux rapidly increased and reached the maximum at a time point of 3 min post-injection and then gradually decreased. The chemiluminescence emission intensity of **SiRCL-1** was ~35-fold stronger at 680 nm than at 540 nm. The obtained results in animal models were consistent in six mice across two independent experiments (Figures S3, S4), demonstrating the validity of using **SiRCL-1** for *in vivo* chemiluminescence imaging.

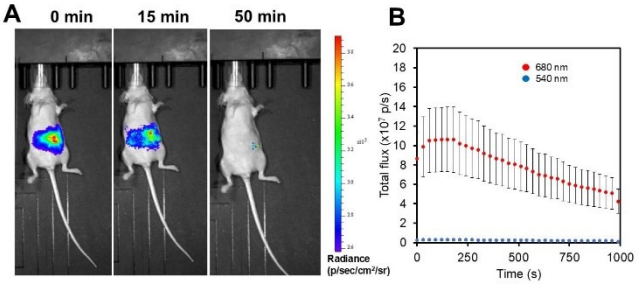

Figure 4. (A) Representative chemiluminescent images of living female mice acquired at 0, 15 and 50 min after intraperitoneal cavity injection of 20 µL **SiRCL-1** (100 µM in 10% DMSO in PBS buffer solution (10 mM, pH=7.4) at 680 nm in an IVIS Spectrum. (B) Emission intensity over time at 540 nm and 680 nm *in vivo* with 10 sec exposure times. Error bars are ± S.E.M. with n = 6 mice across two independent experiments.

Conclusions

In summary, we have developed a near-infrared chemiluminophore silicon rhodamine, **SiRCL-1,** based on CIEEL decomposition and intramolecular energy transfer and demonstrated *in vivo* imaging capability. **SiRCL-1** shows strong response at biological pH, with a remarkable tissue penetration depth greater than 30 mm and long-lived and sustained chemiluminescence emission of greater than 50 min *in vivo*, making it competitive with previously reported NIR chemiluminescence scaffolds (Table S1). The demonstration that **SiRCL-1** undergoes efficient energy transfer, has impressive performance in tissue, and shows suitable aqueous quantum yield make it an attractive candidate for future analyte-specific NIR chemiluminescent sensors.

Author Contributions

Project administration, Funding acquisition, Supervision, and Conceptualization was performed by A.R.L. and R.P.M. Methodology, Investigation, and Analysis were performed by R.O, U.H., M.C., and T.B.D. Original drafting was written by U.H., M.C., and A.R.L. Review and editing was performed by R.O., U.H., M.C., R.P.M., and A.R.L.

Conflicts of interest

A.R.L. declares a financial stake in BioLum Sciences, LLC.

Acknowledgements

The financial support from the National Science Foundation (CHE 2155170, CHE 1653474) and Welch Research Foundation (N-2038-20200401) is acknowledged. Optical imaging was performed in the Small Animal Imaging Shared Resource of the Simmons Cancer Center using an IVIS Spectrum purchased under NIH 1S10RR024757 and supported by NIH P30 CA142543 and CPRIT RP210099.

References

1 M. Vacher, I. Fdez. Galván, B.-W. Ding, S. Schramm, R. Berraud-Pache, P. Naumov, N. Ferré, Y.-J. Liu, I. Navizet, D. Roca-Sanjuán, W. J. Baader and R. Lindh, *Chem. Rev.*, 2018, **118**, 6927–6974.

2 U. Haris, H. N. Kagalwala, Y. L. Kim and A. R. Lippert, *Acc. Chem. Res.*, 2021, **54**, 2844–2857.

3 N. Hananya and D. Shabat, *ACS Cent. Sci.*, 2019, **5**, 949–959.

4 U. Haris and A. R. Lippert, *ACS Sens.*, 2023, **8**, 3–11.

5 M. Yang, J. Huang, J. Fan, J. Du, K. Pu and X. Peng, *Chem. Soc. Rev.*, 2020, **49**, 6800–6815.

6 R. Blau, O. Shelef, D. Shabat and R. Satchi-Fainaro, *Nat. Rev. Bioeng.*, 2023, **1**, 648–664.

7 J. Cao, R. Lopez, J. M. Thacker, J. Y. Moon, C. Jiang, S. N. S. Morris, J. H. Bauer, P. Tao, R. P. Mason and A. R. Lippert, *Chem. Sci.*, 2015, **6**, 1979–1985.

8 L. Liu and R. P. Mason, *PLoS ONE*, 2010, **5**, e12024.

9 A. R. Lippert, *ACS Cent. Sci.*, 2017, **3**, 269–271.

10 O. Green, T. Eilon, N. Hananya, S. Gutkin, C. R. Bauer and D. Shabat, *ACS Cent. Sci.*, 2017, **3**, 349–358.

11 C. Ozsan, K. Kailass, E. M. Digby, T. Almammadov, A. A. Beharry and S. Kolemen, *Chem. Commun.*, 2022, **58**, 10929–10932.

12 B. J. Bezner, L. S. Ryan and A. R. Lippert, *Anal. Chem.*, 2020, **92**, 309–326.

13 M. C. Cabello, G. Chen, M. J. Melville, R. Osman, G. D. Kumar, D. W. Domaille and A. R. Lippert, *Chem. Rev.*, 2024, **124**, 9225–9375.

14 H. Gunduz, A. Acari, S. Cetin, T. Almammadov, N. Pinarbasi-Degirmenci, M. Dirak, A. Cingoz, E. Kilic, T. Bagci-Onder and S. Kolemen, *Sens. Actuators B Chem.*, 2023, **383**, 133574.

15 H. Gunduz, T. Almammadov, M. Dirak, A. Acari, B. Bozkurt and S. Kolemen, *RSC Chem. Biol.* 2023, **4**, 675–684.

16 K. A. Jones, K. Kentala, M. W. Beck, W. An, A. R. Lippert, J. C. Lewis and B. C. Dickinson, *ACS Cent. Sci.* 2019, **5**, 1768–1776.

17 W. An, R. P. Mason and A. R. Lippert, *Org. Biomol. Chem.*, 2018, **16**, 4176–4182.

18 L. S. Ryan, J. Gerberich, U. Haris, D. Nguyen, R. P. Mason and A. R. Lippert, *ACS Sens.*, 2020, **5**, 2925–2932.

19 L. S. Ryan, J. Gerberich, J. Cao, W. An, B. A. Jenkins, R. P. Mason and A. R. Lippert, *ACS Sens.*, 2019, **4**, 1391–1398.

20 H. N. Kagalwala, J. Gerberich, C. J. Smith, R. P. Mason and A. R. Lippert, *Angew. Chem. Int. Ed.*, 2022, **61**, e202115704.

21 S. Gutkin, R. Tannous, Q. Jaber, M. Fridman and D. Shabat, *Chem Sci*, 2023, **14**, 6953–6962.

22 E. A. Mason, R. Lopez and R. P. Mason, *Opt. Mater. Express*, 2016, **6**, 1384–1392.

23 A. K. East, M. Y. Lucero and J. Chan, *Chem. Sci.*, 2021, **12**, 3393–3405.

24 O. Green, S. Gnaim, R. Blau, A. Eldar-Boock, R. Satchi-Fainaro and D. Shabat, *J. Am. Chem. Soc.*, 2017, **139**, 13243–13248.

25 J. Huang, Y. Jiang, J. Li, J. Huang and K. Pu, *Angew. Chem. Int. Ed.*, 2021, **60**, 3999–4003.

26 H. N. Kagalwala and A. R. Lippert, *Angew. Chem. Int. Ed.*, 2022, **61**, e202210057.

27 H. N. Kagalwala, L. Bueno, H. Wanniarachchi, D. K. Unruh, K. B. Hamal, C. I. Pavlich, G. J. Carlson, K. G. Pinney, R. P. Mason and A. R. Lippert, *Analysis & Sensing*, 2023, **3**, e202200085.

28 X. Wei, C. Xu, P. Cheng, Y. Hu, J. Liu, M. Xu, J. Huang, Y. Zhang, and K. Pu, *J. Am. Chem. Soc.*, 2024, **146**, 17393-17403.

29 G. Ma, M. Dirak, Z. Liu, D. Jiang, Y. Wang, C. Xiang, Y. Zhang, Y. Luo, P. Gong, L. Cai, S. Kolemen and P. Zhang, *Angew. Chem. Int. Ed.,* 2024, **63**, e202400658.

30 X. Ni, X. Zhang, X. Duan, H. L. Zheng, X. S. Xue and D. Ding, *Nano Lett.* 2019, **19**, 318−330.

31 J. Li, Y. Hu, Z. Li, W. Liu, T. Deng and J. Li, *Anal. Chem.*, 2021, **93**, 10601–10610.

32 N. Hananya, A. Eldar Boock, C. R. Bauer, R. Satchi-Fainaro and D. Shabat, *J. Am. Chem. Soc.*, 2016, **138**, 13438–13446.

33 S. Vertueux, A. Haefele, K. Solmont, P. Durand and P.Y. Renard, *Eur. J. Org. Chem.* 2023, **26**, e202201401.

34 M. Fu, Y. Xiao, X. Qian, D. Zhao and Y. Xu, *Chem. Commun.*, 2008, 1780–1782.

35 Y. Koide, Y. Urano, K. Hanaoka, T. Terai and T. Nagano, *ACS Chem. Biol.*, 2011, **6**, 600–608.

36 R. J. Iwatate, M. Kamiya, K. Umezawa, H. Kashima, M. Nakadate, R. Kojima and Y. Urano, *Bioconjugate Chem.*, 2018, **29**, 241–244.

37 M. Li, C. Wang, T. Wang, M. Fan, N. Wang, D. Ma, T. Hu and X. Cui, *Chem. Commun.*, 2020, **56**, 2455–2458.

38 J. Miao, Y. Huo, H. Shi, J. Fang, J. Wang and W. Guo, *J. Mater. Chem. B*, 2018, **6**, 4466–4473.

39 G. J. Mao, Z. Z. Liang, G. Q. Gao, Y. Y. Wang, X. Y. Guo, L. Su, H. Zhang, Q. J. Ma and G. Zhang, *Anal. Chim. Acta*, 2019, **1092**, 117–125.

40 W. Piao, S. Tsuda, Y. Tanaka, S. Maeda, F. Liu, S. Takahashi, Y. Kushida, T. Komatsu, T. Ueno, T. Terai, T. Nakazawa, M. Uchiyama, K. Morokuma, T. Nagano and K. Hanaoka, *Angew. Chem. Int. Ed.*, 2013, **52**, 13028–13032.

41 Y. Huo, J. Miao, L. Han, Y. Li, Z. Li, Y. Shi and W. Guo, *Chem. Sci.*, 2017, **8**, 6857–6864.

42 Z. Mao, H. Jiang, X. Song, W. Hu and Z. Liu, *Anal. Chem.*, 2017, **89**, 9620–9624.

43 G. J. Mao, Z. Z. Liang, J. Bi, H. Zhang, H. M. Meng, L. Su, Y. J. Gong, S. Feng and G. Zhang, *Anal. Chim. Acta*, 2019, **1048**, 143–153.

44 Y. Koide, Y. Urano, K. Hanaoka, T. Terai and T. Nagano, *J. Am. Chem. Soc.*, 2011, **133**, 5680–5682.

45 T. Egawa, K. Hanaoka, Y. Koide, S. Ujita, N. Takahashi, Y. Ikegaya, N. Matsuki, T. Terai, T. Ueno, T. Komatsu and T. Nagano, *J. Am. Chem. Soc.*, 2011, **133**, 14157–14159.

46 U. Haris, J. T. Plank, B. Li, Z. A. Page and A. R. Lippert, *ACS Cent. Sci.*, 2022, **8**, 67–76.

47 C. V. Stevani, S. M. Silva and W. J. Baader, *Eur. J. Org. Chem.*, 2000, 4037–4046.

48 F. A. Augusto, G. A. de Souza, S. P. de Souza, M. Khalid and W. J. Baader, *Photochem. Photobiol.*, 2013, **89**, 1299–1317.

Data Availability Statement

The data supporting this article have been included as part of the Supplementary Information.